Supplemental Information

Integrated High Performance Microfluidic Organic Analysis Instrument for Planetary and Space Exploration

Anna L. Butterworth*[#1], Matin Golozar[#2,3], Zachary Estlack[3], Jeremy McCauley[1], Richard A. Mathies[1,2] and Jungkyu Kim*[3]

[1]Space Sciences laboratory, University of California Berkeley, Berkeley CA 94720, USA

[2]Chemistry Department, University of California, Berkeley CA 94720, USA

[3]Department of Mechanical Engineering, University of Utah, Salt Lake City, UT 84112, USA

*Address correspondence:
Anna Butterworth (butterworth@berkeley.edu)
or Jungkyu (Jay) Kim (jkim@mech.utah.edu)

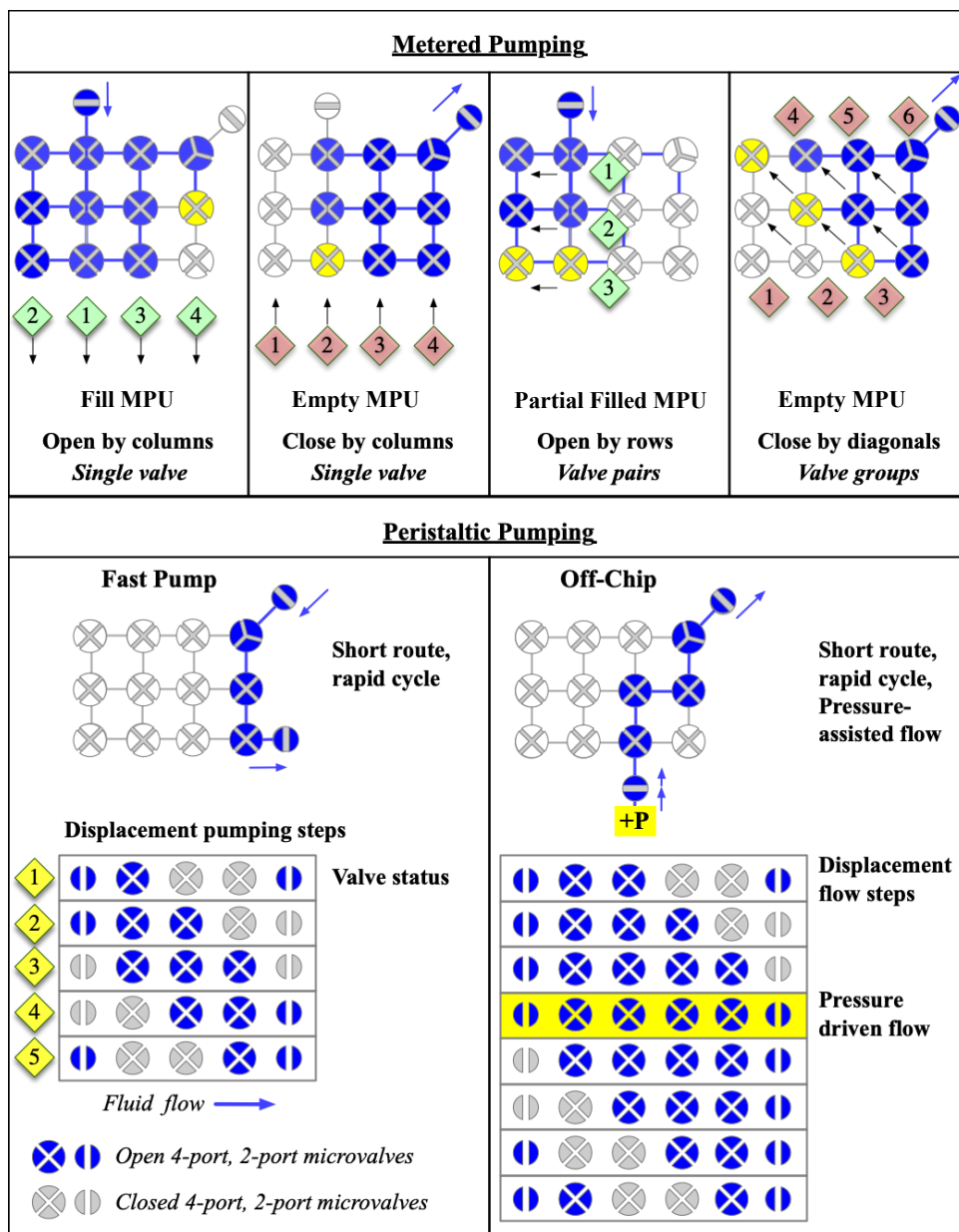[#] These authors contributed equally to this work.

Figure S1. Sequential actuations of the microfluidic processor unit (MPU) enable a wide variety of precise user-defined protocols on the same hardware device. Black arrows denote the order of microvalve actuation during each fluidic step; green diamonds show the order of opening a group of valves (by column, row or diagonal); red diamonds show the order of closing by group; yellow-shaded valves indicate the next actuations in the sequence. The blue arrows show the direction of fluid flow (in or out the MPU array).

Slower filling and emptying of the MPU is used for **metered pumping** for precise volume displacement. A user defined fraction of the MPU valves can be employed to define the fluid volume to be displaced and one-by-one valve actuations provide reliable mixing ratios. Single source processing can employ actuation of 2 or 3 valves switched rapidly as a group to speed up rinsing or priming processes; actuations separated by the 30 ms solenoid switching time are treated as simultaneous with respect to fluid flow control. Times delays between single or group valve actuations are typically 100 to 600 ms.

Lower panel: A fluid bolus is pumped as a wave through a short path in the MPU in **peristaltic pumping**, by switching valve status for each step shown in the table to complete one cycle. Two options are shown for fast on-chip transfer and for ingesting fluid from off-chip using pressure-assisted displacement pumping. In the off-chip example, a "leak" step is inserted (highlighted in yellow), during which all four MPU microvalves and the two routing gate valves open a path directly to the destination allowing pressure driven flow but for less than 1 second per cycle. Adding a small head pressure to the off-chip fluid supply (10 kPa above ambient, well below the breakthrough pressure for the PDMS microvalve structures) overcomes fluid resistance and significantly speeds up the flow, while the displacement pumping provides precision and safety. In this way, off-chip volume and delivery rates are user-defined, without risk of overfilling chip reservoirs.
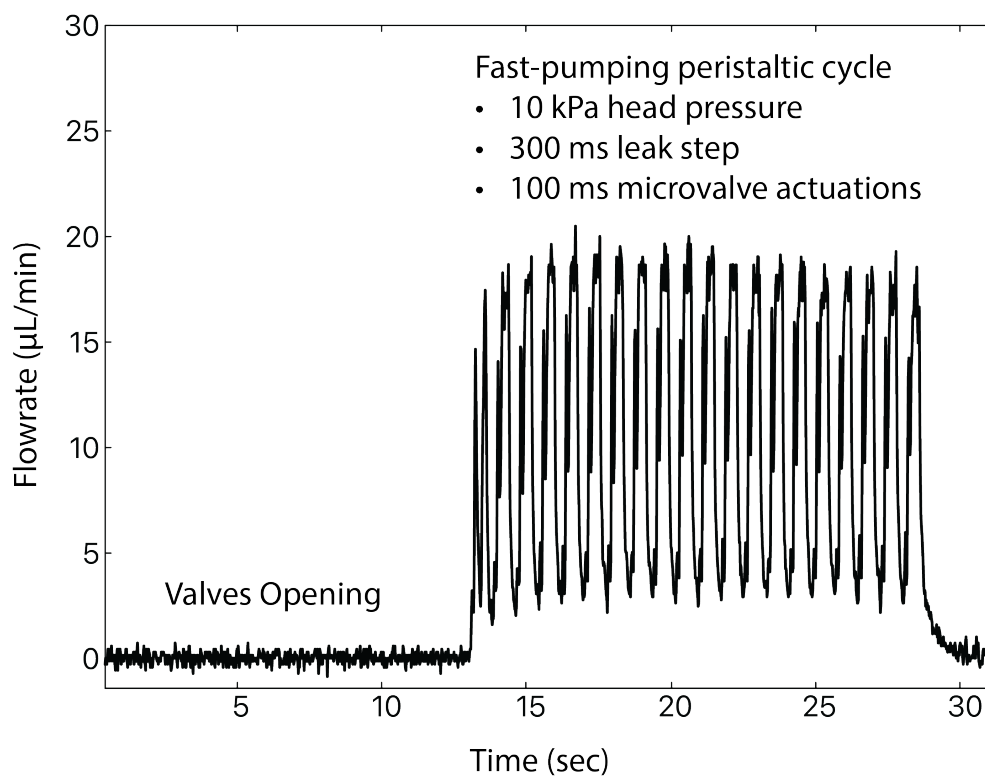

Figure S2. Illustration of the optimized fast-pumping peristaltic cycle, incorporating a 10 kPa head pressure and a 300 ms leakage step, along with 100 ms microvalve actuations, which includes a 30 ms solenoid switching time. This configuration successfully achieves a flow rate of approximately 10 µL/minute. The depicted process is used for drawing fluid from an off-chip source using pressure-assisted displacement pumping. Over a duration of about 17 seconds, the system demonstrates a liquid volume displacement of approximately 2.8 µL.

Detailing the Water Purification and In-Flight Storage Protocols:

As depicted in Figure S3, the initial irradiation stands out as the most effective step, significantly lowering the background levels of impurities. The following distillation phase also plays a vital role in further purifying the sample by decreasing the levels of primary amines, serine, alanine, and glycine. It is important to note a minor increase in background levels, specifically of primary amines, after the final irradiation. This increase is likely due to slight contamination during the transfer process between purification steps, as the water is not fully enclosed and is susceptible to environmental exposure.

For the flight configuration, the storage bellows are equipped with integrated LEDs for in situ purification, which preserves the sterility of the water post-purification by keeping it in a frozen state during the flight. This approach is effective in preventing the introduction and growth of microorganisms, potentially reducing the introduction of amino acids and other organic contaminants. Furthermore, the LEDs can be activated for a final purification step once the water is thawed, just prior to analysis, to eliminate any potential contamination that may have occurred. This ensures the maintenance of water purity right up to the point of utilization in analyses.
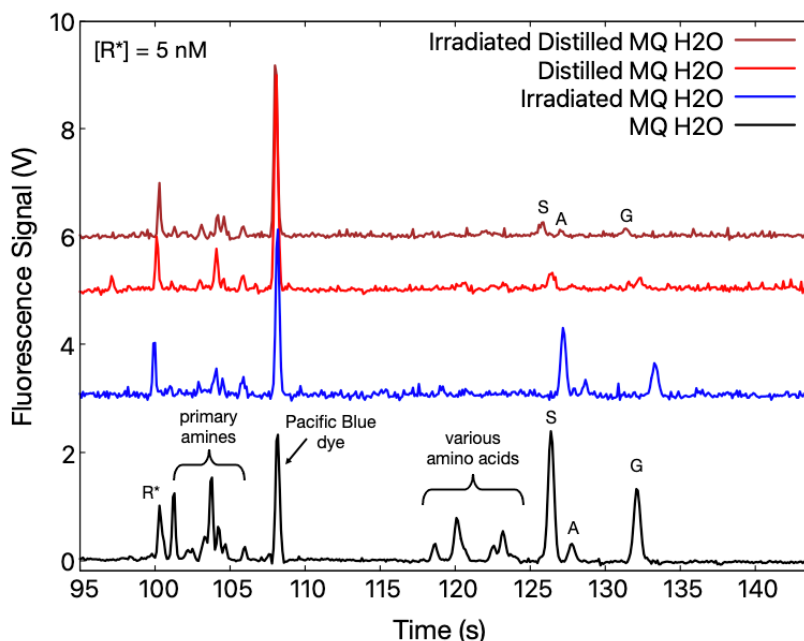

Figure S3. Reduction of Background Amines and Amino Acids Through Purification Process. This electropherogram shows how distillation followed by dual-wavelength UVC irradiation effectively lowers the background levels of primary amines and amino acids in purified water. We used an added 5 nM concentration of arginine as a quantitation standard. The purification process involved irradiating 18.2 MΩ water (Direct-Q, MilliporeSigma) for 12 hours with a UVC lamp emitting at 254 and 185 nm (Black Magic 3D: UVC-25W-OZONE-WT). After initial irradiation, we distilled the water and subjected it to a second round of irradiation to further minimize background amino acids. Residual amino acids—such as Serine at approximately 330 pM, Alanine at around 120 pM, Glycine at close to 240 pM, and primary amines estimated near 770 pM—were detected at sub-nanomolar concentrations. These are most likely introduced as minute impurities originating from the PBSE fluorescent dye, which was present at a 5 μM concentration.
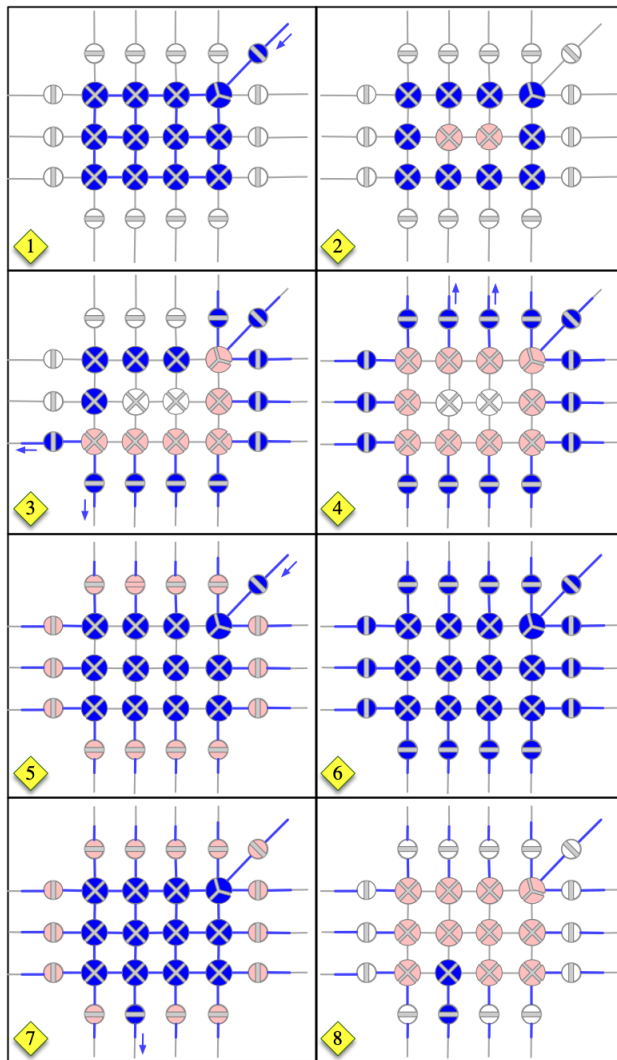
Figure S4. Steps for priming the MPU by pumping in water from *LV1* emptying each time to *Waste* (off-chip). Panel 1: the MPU valves are filled from LV1. Panel 2: preparing to prime the peripheral gate valves, the two central MPU valves are closed. Panels 3 and 4 take 1 second to complete, wherein each remaining MPU valve expels through the attached gate(s). In Panel 5, the gate valves are all closed so that the MPU can be refilled. Panels 2 to 4 are typically repeated 3 times, taking ~30 seconds after which ~200 nL fluid has been pumped to fill each gate valve plus a small length of channel behind each one (preventing air being sucked back to the MPU). In Panel 6, the MPU is held open for 2 minutes to allow the fluid to degas through the PDMS membrane into the vacuum above each valve in the pneumatic layer, taking about 4 minutes total to complete prime the chip from dry until ready for use. Panel 7: It takes 2 seconds to close the gate valves and empty the MPU to Waste, ending with the last valve to close shown in Panel 8, and the chip is ready for immediate use.

Table S1 Automated Sample Preparation and Analysis Steps

Microfluidic Step	Pump Cycle	Repeat	Source	#	Destination	Fill time	Empty time
Priming route with buffer							
Prime Well B1	B6 to B1	1	B6	6	B1	800	400
Prime Well B2	R6B to R2B	1	B6	6	B2	800	400
Prime Well LV1	R6B to LV1	1	B6	12	LV1	800	400
Mix Sample and Dye to label (1:1)							
Mix Sample	B2 to LV1	10	B2	12	LV1	800	400
Mix Dye/Buffer	B1 to LV1		B1	12	LV1	800	400
Dilute labeled sample with CE running buffer (2:3)							
Add Buffer	B6 to LV2	5	B6	12	LV2	800	400
Mix Sample	LV1 to LV2	10	LV1	12	LV2	800	400
Mix Buffer	B6 to LV2		B6	12	LV2	800	400
Transfer labeled sample to CE Sample well							
Transfer to CE	LV2 to CS2	15	LV2	12	CS2	600	400

Vibration Test Reports at 6.8 G_{rms} along X, Y, and Z Directions

Below are the details from our vibration tests executed in the X, Y, and Z axes at an intensity of 6.8 G_{rms}.

- **Breakpoint Table**: This table shows frequency breakpoints alongside their corresponding slopes, expressed in dB per octave. These parameters help to establish the vibration levels at varying frequencies.

- **Test Level Schedule**: This schedule lists out distinct intervals throughout the test. At each interval, specific vibration levels were introduced, followed by observation and documentation.

- **Measurements Section**: This section shows demanded and realized control vibration levels. It also offers measurements for peak-to-peak fluctuations observed in both demanded and controlled vibrations.

- **Channel Measurements**: This section gives measurements for different channels or axes. Data provided captures both the overall and in-band vibration measurements across these channels.

Table S2. Detailed vibration testing results

Along X Direction

Breakpoint table

Frequency	G²/Hz	dB/Octave
20 Hz	0.01	3.01
80 Hz	0.04	0
500 Hz	0.04	-3.01
2000 Hz	0.01	

Test level schedule:

	Duration	Level
1)	0:00:20	-12 dB
2)	View Report	
3)	Wait for operator	
4)	0:00:20	-6 dB
5)	View Report	
6)	Wait for operator	
7)	0:01:00	0 dB
8)	View Report	

** Test started May 21, 2021 18:31:34, running for 0:02:43
** Current level: 7, running at 0 dB for 0:01:00 of 0:01:00

Measurements:

Demand: 6.784 G RMS	0.001173 m pk-pk
Control: 6.775 G RMS	0.001121 m pk-pk

Channel Measurements:

	(Overall)	(InBand)
Control 1	6.589 G RMS	6.588 G RMS
Control 2	6.567 G RMS	6.565 G RMS
OptBase X	10.67 G RMS	10.67 G RMS
Ch4	0.01715 G RMS	0.01709 G RMS
OptBase Y	9.116 G RMS	9.107 G RMS
OptBase Z	4.765 G RMS	4.758 G RMS
Mid X	0.003688 G RMS	0.003135 G RMS
Mid Z	0.003618 G RMS	0.003041 G RMS
Mid Y	0.003645 G RMS	0.003086 G RMS
Top X	0.00377 G RMS	0.003192 G RMS
Top Y	0.003894 G RMS	0.003314 G RMS
Top Z	0.003979 G RMS	0.00341 G RMS

Along Y Direction

Breakpoint table

Frequency	G²/Hz	dB/Octave
20 Hz	0.01	3.01
80 Hz	0.04	0
500 Hz	0.04	-3.01
2000 Hz	0.01	

Test level schedule:

	Duration	Level
1)	0:00:20	-12 dB
2)	View Report	
3)	Wait for operator	
4)	0:00:20	-6 dB
5)	View Report	
6)	Wait for operator	
7)	0:01:00	0 dB
8)	View Report	

** Test started May 21, 2021 18:41:40, running for 0:02:44
** Current level: 7, running at 0 dB for 0:01:00 of 0:01:00

Measurements:

Demand: 6.784 G RMS	0.001173 m pk-pk
Control: 6.781 G RMS	0.001092 m pk-pk

Channel Measurements:

	(Overall)	(InBand)
Control 1	6.571 G RMS	6.57 G RMS
Control 2	6.566 G RMS	6.564 G RMS
OptBase X	4.452 G RMS	4.418 G RMS
Ch4	0.01692 G RMS	0.01685 G RMS
OptBase Y	12.45 G RMS	12.41 G RMS
OptBase Z	8.582 G RMS	8.563 G RMS
Mid X	0.003988 G RMS	0.0035 G RMS
Mid Z	0.003616 G RMS	0.003059 G RMS
Mid Y	0.003618 G RMS	0.003093 G RMS
Top X	0.003738 G RMS	0.003194 G RMS
Top Y	0.003856 G RMS	0.003312 G RMS
Top Z	0.003943 G RMS	0.003411 G RMS

Along Z Direction

Breakpoint table

Frequency	G²/Hz	dB/Octave
20 Hz	0.01	3.01
80 Hz	0.04	0
500 Hz	0.04	-3.01
2000 Hz	0.01	

Test level schedule:

	Duration	Level
1)	0:00:20	-12 dB
2)	View Report	
3)	Wait for operator	
4)	0:00:20	-6 dB
5)	View Report	
6)	Wait for operator	
7)	0:01:00	0 dB
8)	View Report	

** Test started May 21, 2021 17:54:07, running for 0:02:47
** Current level: 7, running at 0 dB for 0:01:00 of 0:01:00

Measurements:

Demand: 6.784 G RMS	0.001173 m pk-pk
Control: 6.78 G RMS	0.001106 m pk-pk

Channel Measurements:

	(Overall)	(InBand)
Control 1	6.511 G RMS	6.499 G RMS
Control 2	6.353 G RMS	6.35 G RMS
OptBase X	4.323 G RMS	4.318 G RMS
Ch4	0.01789 G RMS	0.01783 G RMS
OptBase Y	7.901 G RMS	7.898 G RMS
OptBase Z	14.44 G RMS	14.44 G RMS
Mid X	0.004138 G RMS	0.003668 G RMS
Mid Z	0.003616 G RMS	0.003054 G RMS
Mid Y	0.003743 G RMS	0.003231 G RMS
Top X	0.003892 G RMS	0.003367 G RMS
Top Y	0.004052 G RMS	0.00353 G RMS
Top Z	0.004177 G RMS	0.003674 G RMS

Quantitative Interpretation of Fluorescent Dye Sensitivity Relative to Raman Noise in our Detection System

To quantitatively express the sensitivity of our µPMT and detection system, we carefully measured the inherent Raman shot noise and the signal from a known concentration of Pacific Blue succinimidyl ester (PBSE). The following outlines our calculation procedure:

1. **System Settings**: We used a µPMT gain of 0.8 V, a laser power of 10 mW, and a beam diameter of 55 µm within the detection channel.

2. **Measuring Raman Signal and Noise**:
   - Raman signal was measured at 0.4 V.
   - The associated Raman shot noise was determined to be 1.1e-3 V, calculated using root mean square (RMS) calculations.

3. **Comparing with PBSE Signal**:
   - The signal for 1 nM PBSE was recorded at 0.53 V.
   - The noise for this measurement was 1.3e-3 V.

4. **Background Subtraction and Noise Calculation**:
   - The raw PBSE signal, after subtracting the Raman background, was 0.13 V.
   - The noise after subtraction, calculated using error propagation, was 1.7e-3 V. This was derived using the following equation for the propagation of uncertainty:

$$\delta Q = \sqrt{(\delta a)^2 + (\delta b)^2}$$

where Q represents the final quantity derived from the sums and differences of a and b, and $\delta Q, \delta a, and \ \delta b$ are the respective uncertainties.

5. **Determining Raman Noise Equivalent in PBSE Concentration**:
   - We then determined the equivalent PBSE concentration for the Raman noise using the ratio:

$$\frac{Raman\ Noise\ (V) \times 1\ nM}{1\ nM\ PBSE\ Signal\ (V)}$$

   - This calculation yielded a Raman noise equivalent of approximately 8.5 pM of PBSE.

6. **Limit of Detection (LOD)**:
   - Following standard conventions, the LOD for PBSE was set at a signal-to-noise ratio (SNR) of three, corresponding to approximately 25 pM, based on the Raman noise equivalent.

The summarized data of these measurements, including the calculated Raman noise in PBSE concentration units and the LOD, are presented in Table TS3 for reference.

Table S3 Quantitative Analysis of Raman Noise and Limit of Detection for PBSE

Gain (V)	Raman Signal (V)	Raman Noise (V)	1 nM PB Signal (V)	1 nM PB Noise (V)	BG Subtraction (1 nM PB)	Noise (V)	Raman Noise in pM PB unit	LOD (3X Raman Noise)
0.8	0.40	1.1e-3	0.53	1.3e-3	0.13 V	1.7e-3	8.5 pM	≈ 25 pM